JACS
JOURNAL OF THE AMERICAN CHEMICAL SOCIETY
pubs.acs.org/JACS
Article

Copper(II) Affects the Biochemical Behavior of Proinsulin C-peptide by Forming Ternary Complexes with Serum Albumin

Jessica A. San Juan, Khetpakorn Chakarawet, Zhecheng He, Rebeca L. Fernandez, Michael J. Stevenson, Nathaniel H. O. Harder, Samuel E. Janisse, Lee-Ping Wang, R. David Britt, and Marie C. Heffern*

Cite This: J. Am. Chem. Soc. 2023, 145, 16726−16738

ABSTRACT: Peptide hormones are essential signaling molecules with therapeutic importance. Identifying regulatory factors that drive their activity gives important insight into their mode of action and clinical development. In this work, we demonstrate the combined impact of Cu(II) and the serum protein albumin on the activity of C-peptide, a 31-mer peptide derived from the same prohormone as insulin. C-peptide exhibits beneficial effects, particularly in diabetic patients, but its clinical use has been hampered by a lack of mechanistic understanding. We show that Cu(II) mediates the formation of ternary complexes between albumin and C-peptide and that the resulting species depend on the order of addition. These ternary complexes notably alter peptide activity, showing differences from the peptide or Cu(II)/peptide complexes alone in redox protection as well as in cellular internalization of the peptide. In standard clinical immunoassays for measuring C-peptide levels, the complexes inflate the quantitation of the peptide, suggesting that such adducts may affect biomarker quantitation. Altogether, our work points to the potential relevance of Cu(II)-linked C-peptide/albumin complexes in the peptide's mechanism of action and application as a biomarker.

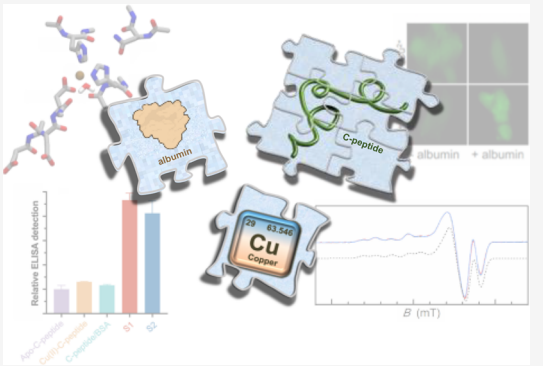

INTRODUCTION

Peptide hormones are key chemical messengers in all forms of life, driving vital functions such as energy homeostasis, reproduction, and stress response.[1] Several FDA-approved drugs have been derived from these hormones, including oxytocin for labor induction and insulin for glucose regulation.[2−4] A number of endogenous peptide hormones have been identified in recent years via combined bioinformatic and structural approaches, but for many of these, their function and mode of action remain elusive.[5] One example is C-peptide, a 31-mer peptide derived from the same prohormone as insulin. Over two decades of research support its physiological effects, including beneficial impacts on glucose uptake, blood flow regulation, and cell growth,[6−9] but its therapeutic advancement has been hindered by a lack of mechanistic understanding,[8] including debate over the identity of its cognate receptor.[10−12] It has been suggested that the elusive activity of the peptide may be due to overlooked regulators and binding partners that modulate function.[8] We and others have recently shown that the activity of C-peptide is influenced by metal ions, warranting further investigations on the molecular bases of these interactions.[13−16]

The signaling activity of bioactive peptides like C-peptide is influenced by the rate of production and secretion, circulation half-life, and the resulting concentration at the target site.[17] Fundamental to the latter two are the potential interactions with plasma proteins. Abundant plasma proteins such as albumin, IgG, and transferrin are versatile carriers of low-molecular metabolites, peptides, and proteins.[18] Serum albumin, in particular, contains four sites where biometals can bind, including one N-terminal site (NTS, Figure S1) containing the classical Amino-Terminal Cu(II)- and Ni(II) (ATCUN) binding motif, a Zn(II) binding site at Cys34, and two multimetal-binding sites: Site A (MBSA, Figure S1), which can bind both Cu(II) and Zn(II), and site B (MBSB) which can bind Zn(II).[19,20] Considering its metal binding capacity, albumin is posited to be the major transporter of endogenous and exogenous metals alike. In addition to metal ions, these binding sites have been investigated for their effects on the bioavailability and distribution of small molecule metallodrugs, including platinum-based anticancer agents.[21,22] Less studied is the chemical nature of how metal-binding peptides may interact with these sites in albumin. In a two-species binding pair model, the high-affinity metal-binding sites on albumin may be considered ligand-exchange competitors for the

Received: May 3, 2023
Published: July 24, 2023

https://doi.org/10.1021/jacs.3c04599
J. Am. Chem. Soc. 2023, 145, 16726−16738

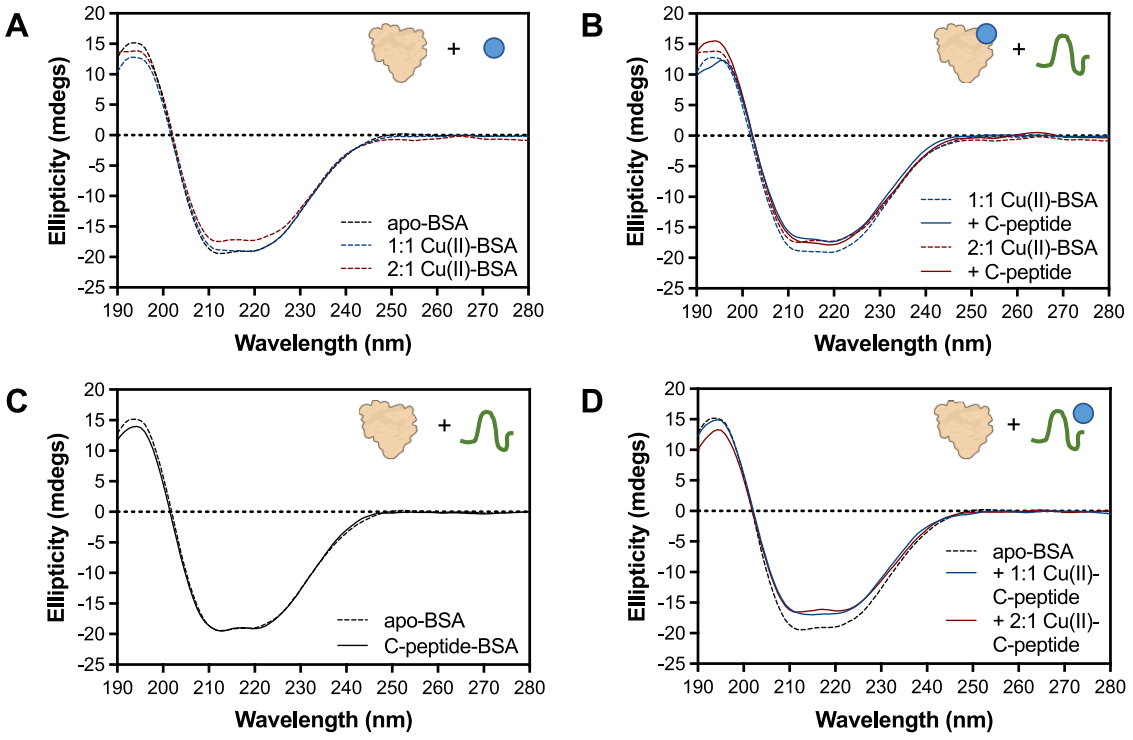

Figure 1. Circular dichroism spectra of 2 μM BSA display structural changes in alpha helicity as shown by shifts in ellipticity at 212 and 222 nm. Inset figures show the associated schemes with BSA (orange protein); Cu(II) (blue circle); C-peptide (green peptide). (A) Minimal reduction of negative ellipticity occurs at 1 equivalent Cu(II), with further reduction at 2 equivalents Cu(II). (B) Addition of apo-C-peptide to 1:1 Cu(II)-BSA shows perturbations in secondary structure, while 2:1 Cu(II)-BSA displays modest shifts. (C) In the absence of Cu(II), the CD spectra of apo-C-peptide and apo-BSA overlaps to the spectra of apo-BSA alone. (D) With the addition of 1:1 and 2:1 Cu(II)−C-peptide to apo-BSA, similar decreases in ellipticity occur.

peptide-bound metal ions. Choi and colleagues recently demonstrated that serum albumin can bind to and sequester metal ions from Zn(II) and Cu(II)-loaded amyloid-beta (Aβ), a peptide implicated in the pathologies associated with Alzheimer's disease. The metal-bound Aβ/albumin interaction affects the peptide's cytotoxicity, pointing to a possible regulatory role of albumin in the metal/Aβ pathophysiology.[23−27] Recently, another binding model between albumin and metal-binding peptides was presented by Bossak-Ahmad et al. with the Cu(II)-containing tripeptide, GHK, namely that the metal center may serve as a bridge in a peptide-metal-albumin ternary complex.[28]

The activity of C-peptide has indeed been linked to both metal ions and the presence of albumin.[13] Spence and co-workers first demonstrated that the activity of C-peptide in modulating blood vessel physiology is activated by the addition of Zn(II).[29,30] Interestingly, the ability of C-peptide to increase GLUT1 levels and ATP release in red blood cells were further elevated by the coaddition of bovine serum albumin (BSA) alongside Zn(II).[13,14] They proposed that the C-peptide receptor may actually recognize the peptide complexed to albumin rather than the peptide alone;[13,14] but the molecular nature of such a complex and whether Zn(II) is involved in its formation require further characterization. We recently demonstrated that Cu(II) can directly bind to C-peptide and alter the cellular internalization of the peptide.[16] We identified that the binding interaction was focused on the N-terminal region of the peptide involving the E3 and D4 residues, forming a 1N3O square-planar Cu(II) complex. While we determined that Zn(II) could also bind to the peptide directly via the peptide backbone, Cu(II) addition displaces the Zn(II). Moreover, the full-length sequence of C-peptide is necessary for precise binding of Cu(II) to C-peptide, with mutations or truncations of the metal-binding region leading to reshuffling of the binding site (Figure S1).[15]

Herein, we sought to assess whether Cu(II) or Zn(II) could facilitate interactions between C-peptide and albumin (using BSA as a model system) and characterize the molecular nature of the species formed. We demonstrate that Cu(II) facilitates the formation of ternary complexes between C-peptide and BSA which do not form in the absence of Cu(II), and that such an interaction is not observed with Zn(II). Interestingly, the resulting complexes depend on the order of addition. Characterization via circular dichroism spectroscopy supports the formation of distinct species when a C-peptide/Cu(II) complex is added to BSA versus when Cu(II)-coordinated BSA is added to C-peptide. We demonstrate the potential clinical relevance of the ternary complexes with their effects on bioanalytical immunoassays for C-peptide. C-peptide is a well-accepted secondary biomarker for insulin as the two are co-released,[31,32] with C-peptide exhibiting a higher circulation lifetime.[33] Our results show that the presence of the ternary complexes significantly affects the read-out in these assays, conveying their potential importance to diagnostic measurements. The ternary complexes also exhibit higher protection of the Cu(II) center from reduction than albumin or C-peptide alone, suggesting a possible metal sequestration function. Within the cellular context, inclusion of serum albumin alters internalization of the peptide into human embryonic kidney cells, with the complexes showing distinct activity from one another. Further spectroscopic characterization of the ternary complexes in conjunction with time-dependent density func-

https://doi.org/10.1021/jacs.3c04599
J. Am. Chem. Soc. 2023, 145, 16726−16738

tional theory (TDDFT) calculations demonstrates that while the ligand set around the Cu(II) center shows close similarity to the Cu(II)-albumin sites, the ternary complexes differ from Cu(II)-albumin and from each other in their global conformations, likely from distinctions in the orientations of C-peptide and albumin about the Cu(II) center. Overall, the presented data point to the impact of these C-peptide/albumin/Cu(II) complexes on the molecular action and clinical applications of C-peptide as well as to the metal-associated roles serum albumin may play in regulating extracellular peptide activity.

RESULTS AND DISCUSSION

Cu(II) Facilitates Interactions between C-peptide and Albumin. We first assayed whether Cu(II) or Zn(II) could facilitate interactions between C-peptide and albumin differently than in the absence of either metal by application of Förster resonance energy transfer (FRET). The FRET phenomenon is widely used in fluorescence spectrophotometry to assess protein−ligand interactions. In these applications, two species of interest are independently labeled with two parts of a FRET pair. FRET efficiency is used to determine if the two species come in close enough proximity (within the Förster distance) for energy transfer to occur.[34] To apply this approach to C-peptide and albumin, we generated C-peptide labeled with the fluorescent dye TAMRA (TAMRA-C-peptide; λ_{ex} = 546 nm, λ_{em} = 579 nm) to be used as a FRET acceptor alongside BSA that has been labeled with fluorescein isothiocyanate (FITC-albumin, λ_{ex} = 495 nm, λ_{em} = 520 nm), an established FRET donor for TAMRA.[35,36] To screen for binding interactions between TAMRA-C-peptide and FITC-albumin, the FRET efficiency was measured with increasing ratios of donor-to-acceptor (See Supporting Discussion 1, Figures S2 and S3). When TAMRA-C-peptide is preincubated with Cu(II), then added to FITC-albumin, an increase in the FRET efficiency is observed with increasing donor-to-acceptor ratios (Figure S2B), suggesting energy transfer through binding between the two species. Such an increase was not observed with the addition of Zn(II) nor in the absence of either metal (Figure S2A and S2C). The data from this assay indicate that Cu(II) may mediate the formation of a C-peptide/albumin complex that does not otherwise occur under the other conditions tested. We thus sought to further characterize the interaction with fluorophore-free forms of the peptide and protein.

Changes to the secondary structure of BSA are frequently used as a proxy for characterizing the binding of drug metabolites and co-factors, including Cu(II) to the protein.[19,37,38] We thus applied circular dichroism (CD) spectroscopy to screen for impacts of Cu(II) on interactions between C-peptide and albumin. The CD spectrum of BSA in the absence of Cu(II) (apo-BSA) exhibits two negative bands at approximately λ = 208 and 222 nm, characteristic of the α-helical structures that make up the protein.[39,40] These negative bands arise from contributions of the $n \rightarrow \pi^*$ transition of a peptide bond within the α-helices of the protein.[41] Under the conditions we tested, the 208 nm band is slightly red-shifted to 212 nm (Figure 1A). We estimated the mean residue ellipticities (MREs) at 212 and 222 nm and their ratios using eq 1

$$\mathrm{MRE}_{212 \text{ or } 222 \text{ nm}} = \frac{\text{observed CD (mdeg)}}{C_p n l \times 10} \quad (1)$$

where C_p is the molar concentration, n is number of amino acid residues, and l is the pathlength. From the MRE, the helical content can be approximated using eq 2:

$$\alpha - \text{helix (\%)} = \frac{\mathrm{MRE} - 4000}{33{,}000 - 4000} \times 100 \quad (2)$$

This method has been used to assess ligand effects on the albumin structure in a semiquantitative manner.[42−44] We estimated the helical content of apo-BSA to be 71.1 and 68.2% at 212 and 222 nm, respectively (Figure 1A, Table 1). Serum albumin can bind up to two equivalents of Cu(II). In buffered solution, it has been shown that addition of one molar equivalent of Cu(II) primarily populates the higher-affinity NTS site, while the addition of two equivalents allows for Cu(II) occupation of both the NTS and MBSA sites;[38] these distinct occupations are observable by detectable differences in the protein's secondary structure.[45] Consistent with the literature,[45,46] we observed that the addition of one equivalent of Cu(II) (1:1 Cu(II)-BSA) induces a modest reduction in negative molar ellipticity at 212 nm (corresponding to an overall 1.8% decrease in helicity), while two equivalents of Cu(II) (2:1 Cu(II)-BSA) induce notable reductions in the negative ellipticity at both 212 and 222 nm (corresponding to an overall 5.7% and 4.9% decrease in helicity) (Figure 1A, Table 2).

Table 1. Alpha Helical Content for BSA with the Addition of Apo-C-peptide or 1 and 2 Equivalents of Cu(II)−C-peptide[a]

Wavelength (nm)	Apo-BSA	Apo-BSA + Apo-C-peptide	Apo-BSA + 1:1 Cu(II)−C-peptide	Apo-BSA + 2:1 Cu(II)−C-peptide
212	71.1 ± 0.1	71.1 ± 0.2	63.1 ± 0.3	62.7 ± 0.1
222	68.2 ± 0.4	69.2 ± 0.4	62.5 ± 0.2	61.7 ± 0.2

[a]Data reported as mean ± SD with n = 3.

Table 2. Alpha Helical Content for BSA with the Addition of 1 and 2 Equivalents of Cu(II), Followed by the Addition of Apo-C-peptide[a]

Wavelength (nm)	1:1 Cu(II)-BSA	1:1 Cu(II)-BSA + Apo-C-peptide	2:1 Cu(II)-BSA	2:1 Cu(II)-BSA + Apo-C-peptide
212	69.3 ± 0.1	62.8 ± 0.3	65.4 ± 0.2	64.4 ± 0.4
222	68.3 ± 0.3	63.4 ± 0.5	63.3 ± 0.4	64.9 ± 0.4

[a]Data reported as mean ± SD with n = 3.

In the absence of BSA, the CD spectra of metal-free C-peptide (apo-C-peptide) and 1:1 or 2:1 Cu(II)−C-peptide represent primarily random coil conformations with no detectable helical content (Figure S4). When apo-C-peptide is added to apo-BSA, the resulting CD spectral traces and helical content closely overlap with apo-BSA at both the 212 and 222 nm peak regions (Figure 1C and Table 1). This suggests that the molar ellipticity of apo-C-peptide is minimally detectable in the presence of apo-BSA, and that the two species do not interact in a way that perturbs the secondary structure of apo-BSA. We next compared the spectra and helicity values of apo-BSA, 1:1 Cu(II)-BSA, and 2:1 Cu(II)-BSA and the

https://doi.org/10.1021/jacs.3c04599
J. Am. Chem. Soc. 2023, 145, 16726−16738

resulting spectra and values upon addition of C-peptide. In contrast to the addition of apo-C-peptide to apo-BSA, addition of apo-C-peptide to 1:1 Cu(II)-BSA decreases the helical content at 212 and 222 nm by 6.5 and 4.9% respectively relative to 1:1 Cu(II)-BSA alone (Figure 1B, Table 2). The helicity content of 2:1 Cu(II)-BSA at 212 and 222 nm similarly shifts in the presence of C-peptide albeit to a lesser degree than at 1:1 Cu(II)-BSA (an overall 1% decrease and 1.6% increase, respectively, over 2:1 Cu(II)-BSA alone) (Figure 1B, Table 2). These shifts indicate that addition of apo-C-peptide to Cu(II)-BSA at either Cu(II) equivalent, may result in the formation of new species that are distinct from Cu(II)-BSA alone.

As we had previously observed direct binding of Cu(II) to C-peptide ($K_{d,\ Cu(II)/C\text{-}peptide}$ = 10 nM at pH 7.4),[15] we investigated whether similar shifts in the apo-BSA structure could be observed if Cu(II) pre-complexed to C-peptide at 1 or 2 equivalents (1:1 Cu(II)−C-peptide or 2:1 Cu(II)−C-peptide) was introduced to apo-BSA. Our prior work with C-peptide supports the binding of at least 1 equivalent of Cu(II);[16] while we did not elucidate the nature of the second binding site, we observed that mutating or truncating the binding site of the first Cu(II) does not eradicate, but rather, reshuffles the binding site, pointing to a possibility of the peptide binding a second Cu(II) equivalent.[15] We thus pre-incubated C-peptide with Cu(II) at both one or two equivalents prior to addition to apo-BSA and the CD spectra were monitored and compared to apo-BSA alone. The addition of 1:1 and 2:1 Cu(II)−C-peptide to apo-BSA reduces the negative ellipticity of apo-BSA. Relative to apo-BSA, addition of 1:1 Cu(II)−C-peptide notably decreases the helical content at 212 and 222 nm by 8 and 5.7%, respectively, while the addition of 2:1 Cu(II)−C-peptide decreases helical content further at 212 and 222 nm by 8.4 and 6.5% (Figure 1D, Table 2). Of note, the resulting CD spectra when 1:1 and 2:1 Cu(II)−C-peptide are added to apo-BSA are distinct from the CD spectra of the addition of apo-C-peptide to Cu(II)-BSA at the corresponding Cu(II) equivalents.

Under every condition where C-peptide, Cu(II), and BSA are all present, the CD data point to the ability of Cu(II) to mediate complex formation between C-peptide and BSA that otherwise does not occur in the absence of the metal ion. Moreover, the order of addition—whether Cu(II) is first loaded into the peptide then added to the protein, or first to the protein prior to peptide addition—affects the formation of the resulting species. Thus we identify two scenarios by which spectroscopically distinct C-peptide/BSA/Cu(II) ternary complexes may form (Table 3): either C-peptide binds to metalated sites on Cu(II)-BSA (C-peptide + Cu(II)-BSA) or pre-formed Cu(II)−C-peptide complexes coordinate to BSA (Cu(II)−C-peptide + BSA).

Formation of Ternary Species Inflates C-peptide Measurements. Perhaps the most widespread clinical application of C-peptide to date is as a secondary biomarker for insulin,[31,32] given that the two are coreleased from the pancreas and C-peptide bears a significantly longer half-life.[33] As we demonstrated that C-peptide may associate with albumin in copper-linked complexes, we investigated whether the formation of these species would affect the measurement of C-peptide levels with a standard clinical immunoassay. The C-peptide enzyme-linked immunosorbent assay (ELISA) measures C-peptide by immobilized immunoaffinities of the peptide. We compared the detection of C-peptide in its apo-form to the addition of Cu(II), BSA, and the C-peptide/BSA/

Table 3. Schematic Representations of Experimental Setups and Corresponding Nomenclature in this work[a]

Nomenclature	Experimental Scheme
Cu(II)-C-peptide	
Cu(II)-BSA	
C-peptide + Cu(II)-BSA	
Cu(II)-C-peptide + BSA	

[a]Cu(II) facilitates the formation of ternary complexes with C-peptide and BSA. The order of addition—whether Cu(II) is preincubated with C-peptide first then added to BSA (Cu(II)−C-peptide + BSA) or C-peptide is added to a pre-complexed mixture of Cu(II) and BSA (C-peptide + Cu(II)-BSA)—affects the structure of the resulting species.

Cu(II) complexes. The presence of either Cu(II) or albumin does not significantly affect the ELISA-based detection of C-peptide. However, when all biomolecules are present either via the C-peptide + Cu(II)-BSA or as Cu(II)−C-peptide + BSA preparations, the ELISA registers significantly higher C-peptide levels than was added into the solution, showing 4.7- and 4.1-fold increases in measured C-peptide levels, respectively (Figure 2). In contrast, the addition of Zn(II) following these same conditions does not significantly shift ELISA-based detection of C-peptide (Figure S5). Altogether, these observations suggest that the presence of these ternary complexes may affect biomarker quantification. These

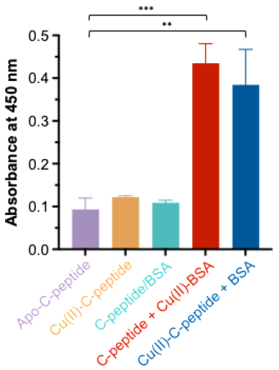

Figure 2. C-peptide ELISA (abs. at 450 nm) for detecting C-peptide by antibody recognition in solutions containing 50 pg/mL of apo-C-peptide, Cu(II), and BSA. Measurements were done in biological replicates (n = 3), and ELISA detection was normalized to apo-C-peptide. The presence of Cu(II) (orange) or BSA (teal) with C-peptide minimally shifts C-peptide detection. When C-peptide is added to Cu(II)-BSA (red) or when Cu(II)-C-peptide is added to BSA (blue), C-peptide detection significantly increases. Significance is analyzed by the unpaired t-test; $^{**}p < 0.01$, $^{***}p < 0.005$. Data are shown as mean ± SD with n = 3.

https://doi.org/10.1021/jacs.3c04599
J. Am. Chem. Soc. 2023, 145, 16726−16738

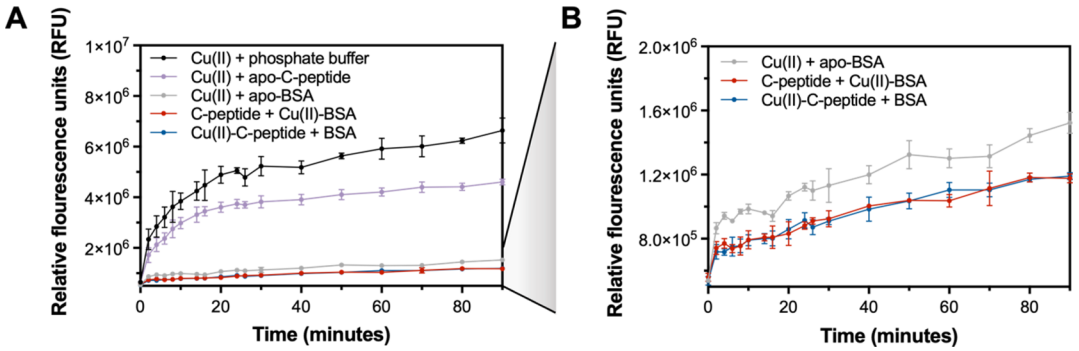

Figure 3. Fluorescent 7-OH-CCA assay (ex. 338 nm, em. 450 nm) for measuring redox protection from Cu(II)-induced $OH^{\cdot}$ generation by solutions containing 2 μM Cu(II) in the presence or absence of 2 μM C-peptide and/or BSA in 10 mM phosphate buffer at pH 7.4. (A) RFU of C-peptide decreases in comparison to phosphate buffer, but not to the same extent as either BSA or the ternary complexes. (B) Inset of (A) highlights that C-peptide + Cu(II)-BSA and Cu(II)−C-peptide + BSA show increased redox protection as compared to Cu(II)-BSA. Data are shown as mean ± SD with n = 3.

complexes warrant further consideration both in terms of their impact on diagnoses and treatment regimens and their chemical and biological behavior.

Ternary Complexes Modify Cu(II) Redox Behavior. Cu(II) coordination to peptides has been previously shown to alter the metal ion's redox susceptibility relative to its "free" aquated form.[47,48] In addition, both Cu(II) and C-peptide have independently been shown to impact oxidative balance within biological systems.[7,8,47,48] Thus, we assessed and compared the ability of C-peptide, BSA, and the ternary complexes to affect the Fenton-type chemistry of Cu(II). In its "free" form (i.e., the addition of $CuCl_2$ to a buffered aqueous solution), Cu(II) ions in solution are reduced to Cu(I) when exposed to a reducing agent such as ascorbic acid (eq 3). In the presence of dissolved O_2, the resulting Cu(I) can catalyze the production of reactive oxygen species (ROS) such as $OH^{\cdot}$ radicals via Fenton-type reactions (eqs 4−6).

$$\text{Ascorbic Acid} + \text{Cu(II)} \rightarrow \text{Dehydroascorbic Acid} + \text{Cu(I)} \quad (3)$$

$$\text{Cu(I)} + \text{O}_2 \rightarrow \text{Cu(II)} + \text{O}_2^{-} \quad (4)$$

$$2\text{O}_2^{-} + 2\,\text{H}^{+} \rightarrow \text{H}_2\text{O}_2 + \text{O}_2 \quad (5)$$

$$\text{Cu(I)} + \text{H}_2\text{O}_2 \rightarrow \text{Cu(II)} + \text{HO}^{-} + \text{HO}^{\cdot} \quad (6)$$

In this way, ROS production by Cu(II) reduction has been used as an indicator of Cu(II) ion availability in solution. Nonfluorescent coumarin-3 carboxylic acid (3-CCA) is oxidized to fluorescent 7-OH-CCA (excitation at 388 nm, emission at 450 nm) in the presence of $HO^{\cdot}$ radicals and has been applied as a probe for ROS production.[47,48] We evaluated the ability of C-peptide, BSA, and the ternary complexes to affect reduction of the Cu(II) ion by ascorbic acid via 7-OH-CCA fluorescence (Figure 3). To simplify the comparison of the various Cu(II)-containing species, the amount of "free" Cu(II) ions in solution under the various conditions were minimized by limiting studies to one molar equivalent of Cu(II). In comparison to Cu(II) salt in phosphate buffer, Cu(II)−C-peptide exhibits decreased formation of 7-OH-CCA, indicating that the peptide decreases free Cu(II) availability (Figure 3A). Cu(II)-BSA further reduces 7-OH-CCA formation to a more appreciable extent than C-peptide, suggesting a higher degree of Cu(II) redox protection in Cu(II)-BSA. Intriguingly, the ternary complexes further reduce the 7-OH-CCA as compared to Cu(II)-BSA (Figure 3B). The degrees of redox protection of the ternary species appear similar between the two orders of addition. However, we note that the low levels of 7-OH-CCA fluorescence generated may put the measurements below the detection limit to distinguish the two species. These data suggest that the combined presence of Cu(II), BSA, and C-peptide generates Cu(II)-containing species with distinct, elevated redox protection than either Cu(II)−C-peptide or Cu(II)-BSA.

Cu(II) and Albumin Combined Modify the Cellular Behavior of C-peptide. Unlike classical peptide hormones, C-peptide is internalized into HEK-293 (human embryonic kidney) cells via endocytosis.[49] We previously showed that Cu(II) affects the peptide's behavior in cells, wherein the addition of a slight excess of Cu(II) (11 μM $CuCl_2$ to 10 μM peptide) decreases this internalization.[16] To determine whether the Cu(II)-containing C-peptide/BSA complexes have biological relevance in the cellular context, we assessed whether the combined presence of Cu(II) and albumin could impact peptide internalization. An important consideration in these studies is that the addition of BSA alone to cells cultured in serum-free media prominently affects cell growth.[50] As complexation of BSA to either copper, C-peptide, or both may affect the available cell concentrations, BSA was applied in excess (10-fold) to C-peptide to maintain consistent cell growth across conditions and focus analysis on the effects of the ternary species on C-peptide internalization. We also further reasoned that providing BSA in excess would ensure that the available C-peptide in the media would be bound in the ternary complex to distinguish internalization behavior from C-peptide in the absence of albumin and/or Cu(II). Due to differences in cell growth, comparisons could only be made between samples that had equal amounts (0 or 100 μM) of BSA and not between samples with differing amounts of BSA.

All cells were cultured and plated in the presence of serum, then starved of serum overnight. For BSA-absent conditions, cells were treated with serum-free media containing either vehicle (media only), C-peptide alone (apo-C-peptide), or 11 μM Cu(II) combined with 10 μM C-peptide (termed Cu(II)−C-peptide per Table 3). For BSA-present conditions, serum-free media supplemented with 100 μM BSA was used as the treatment vehicle, and cells were treated with either vehicle alone, apo-C-peptide, and apo-C-peptide in the BSA-containing treatment media that had been preincubated with 11 μM Cu(II) (termed C-peptide + Cu(II)-BSA per Table 3),

https://doi.org/10.1021/jacs.3c04599
J. Am. Chem. Soc. 2023, 145, 16726−16738

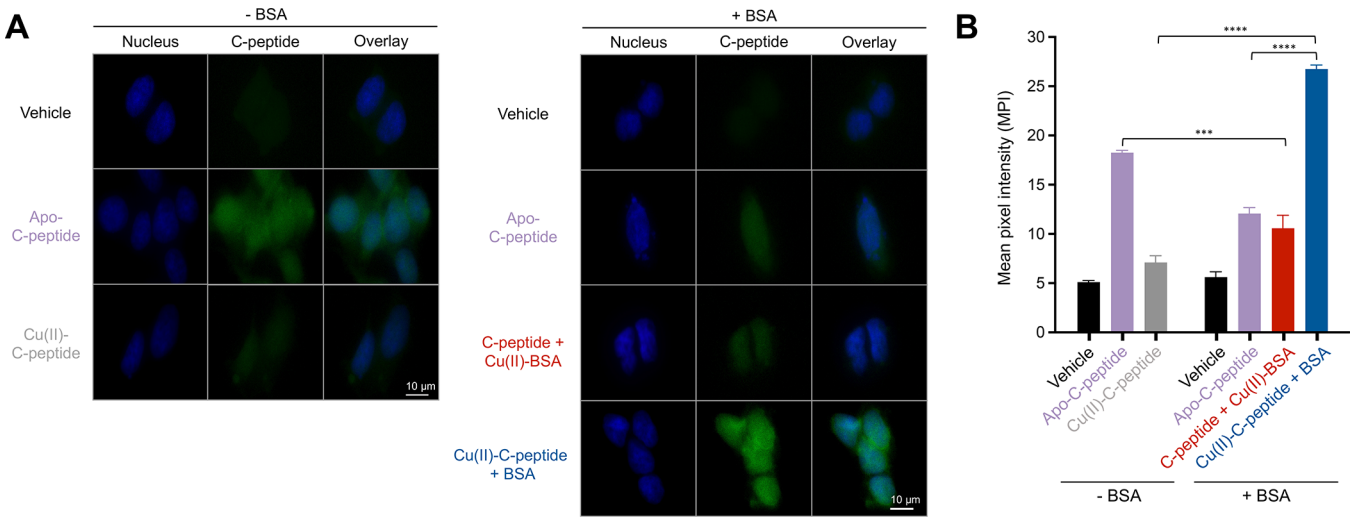

Figure 4. Immunofluorescence imaging of C-peptide uptake into HEK-293 cells when stimulated with 10 μM C-peptide, 11 μM $CuCl_2$, in the absence (−BSA) or presence (+BSA) of 100 μM BSA. (A) Fixed cells were immunolabeled with C-peptide primary antibodies followed by secondary antibodies conjugated to Alexa Fluor 488. (B) Comparisons of fluorescence intensity of Alexa Fluor 488 immuno-labeled C-peptide. Data represent mean pixel intensities in regions of interest as mean ± SD with $n = 3$. Significance is analyzed by the unpaired t-test; ***$p < 0.005$, ****$p < 0.0001$. In BSA-absent conditions (− BSA), uptake of Cu(II)-C-peptide is lower in comparison to apo-C-peptide. In contrast, in BSA-present conditions (+ BSA), preincubating the C-peptide with Cu(II) (Cu(II)−C-peptide + BSA) yields a dramatic increase in C-peptide internalization that is not observed when Cu(II) is added to the media first, followed by C-peptide (C-peptide + Cu(II)-BSA).

or a preincubated solution of C-peptide and Cu(II) (termed Cu(II)-C-peptide + BSA per Table 3). To detect peptide uptake, cells were fixed, permeabilized, and incubated with C-peptide primary antibodies, followed by secondary antibodies conjugated with Alexa Fluor 488 fluorophore (Figure 4A). Mean pixel intensities of each sample condition were used to determine shifts in C-peptide internalization (Figure 4B). Consistent with previous studies, the presence of Cu(II) in BSA-absent media leads to a decrease in internalization of C-peptide. In contrast, under BSA-present conditions, the preincubation of Cu(II)−C-peptide results in a marked increase in peptide internalization (Figure 4A,B) relative to apo-C-peptide. The data confirms that the combined presence of albumin and Cu(II) differentially impacts C-peptide internalization. Interestingly, if the albumin-containing media is pretreated with Cu(II), the same enhancement in C-peptide internalization is not observed (Figure 4, C-peptide + Cu(II)-BSA). The distinct cellular behavior that arises with differential order of addition supports the observations from the CD spectroscopic studies, namely, that the structures of the ternary complexes that form are influenced by the order of addition of the three species. Importantly, the resulting difference in cellular internalization suggest that the species that forms may strongly impact the activity of the peptide.

When the analogous experiments are performed with Zn(II) instead of Cu(II) (Figure S6A and S6B), a similar enhancement in peptide internalization is observed when cells are treated with Zn(II) preincubated with C-peptide under BSA-present conditions. While a decrease in internalization of Zn(II)−C-peptide is also observed relative to apo-C-peptide under BSA-absent conditions, the decrease is modest when compared to the effects of Cu(II) and shows no statistical significance. The cellular effects of Zn(II) on C-peptide internalization in BSA-present conditions is intriguing given that neither the FRET-based assay nor the ELISA quantification are impacted by Zn(II). It is possible that the effects are occurring independent of a ternary complex detectable via FRET-based assay (Figure S2C), warranting additional studies on the molecular regulation of the Zn(II)/C-peptide/albumin interaction.

The uptake pathways that initiate the cellular activity of C-peptide remain elusive as several internalization methods have been proposed but not substantiated at the molecular level—passive diffusion, receptor-independent endocytosis, and receptor-dependent endocytosis.[49,51,52] Previous studies have shown that under stress conditions, albumin can internalize into cells via endocytosis.[53] This supports Spence and coworkers' hypothesis that the C-peptide receptor may interact with the peptide complexed to albumin and not the peptide alone.[13,14] The immunofluorescence data point to the possibility that copper-stabilization of a C-peptide complex with albumin may direct uptake of the peptide via an albumin-associated pathway and that this pathway may diverge when cells are treated with the peptide in the absence of albumin. As debate remains whether C-peptide uptake is receptor-mediated, and if so, which receptor serves as the peptide's cognate, additional work is required to fully elucidate the impact of metal ions on cellular activity. However, our work suggests the potential importance of considering metal ions as mediators of C-peptide signaling, and their inclusion into future studies may better facilitate our understanding of the peptide's mode of action.

Order and Equivalence of Cu(II) Produce Distinct Metal Coordination Sites. The results from the presented in vitro assays, biochemical measurements, and cellular studies all point to the Cu(II)-dependent formation of distinct complexes between C-peptide and albumin. Moreover, both the CD and cellular studies suggest that the order by which Cu(II) is added into the mixture affects the resulting species. We sought to further characterize these ternary complexes by assessing the Cu(II) coordination environment in comparison to Cu(II)−C-peptide and Cu(II)-BSA. We investigated the Cu(II) sites using the d−d region in the electronic absorption spectra, which is sensitive to coordination geometry and ligand

https://doi.org/10.1021/jacs.3c04599
J. Am. Chem. Soc. 2023, 145, 16726−16738

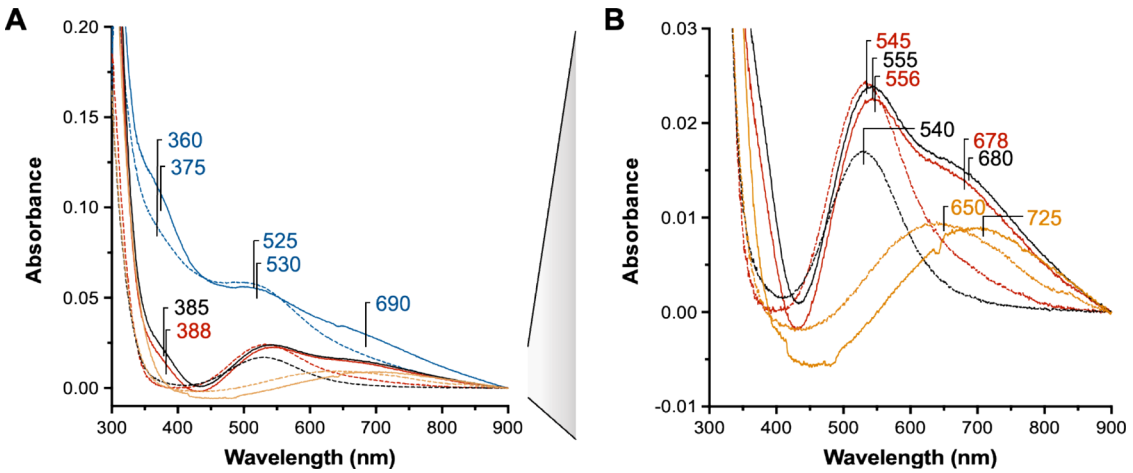

Figure 5. UV−Visible spectra of Cu(II)−C-peptide (orange), Cu(II)-BSA (black), C-peptide + Cu(II)-BSA (red), and Cu(II)−C-peptide + BSA (blue) at one (dashed line) and two (solid line) equivalents of Cu(II). Samples were prepared in 10 mM phosphate buffer at pH 7.4 with 300 μM C-peptide, 300 μM BSA, and/or either 300 μM (1 equivalent) or 600 μM (2 equivalents) $CuCl_2$. Absorbance values are reported as the values when subtracted from the spectra of the same mixture but in the absence of Cu(II) to facilitate analysis of the d-d bands. The spectra prior to subtraction are shown in Figure S8A. (A) Overlay display of all subtracted spectra in the 300−900 nm range, alongside an (B) inset to highlight subtle blue- or red-shifts in wavelength in the 500−700 nm range.

identity. As described in previous reports[38,46] and our CD studies, the loading of Cu(II) into the two sites of BSA can be spectroscopically distinguished in buffered solution by varying the equivalents of Cu(II). Specifically, the high-affinity N-terminal site (NTS, K_d = 1 pM) is the primary site of metalation at one equivalent of Cu(II) while addition of two equivalents populates both the NTS site and the lower-affinity Multimetal-binding site A (MBSA, K_d = 10 nM[19] at pH 7.4 in phosphate buffer). We observe that the population of the NTS with copper (1:1 Cu(II)-BSA) yields a d−d band with λ_{max} at 540 nm (Figure 5B, Table 4, and Figure S7), characteristic of a strong square-planar ligand field.[38,46] Further addition of Cu(II) (2:1 Cu(II)-BSA) produces a red-shifted band with λ_{max} at 555 nm, a charge transfer (CT) transition band at 385 nm, and a second band with λ_{max} at 680 nm (Figure 5A,B, Table 5, and Figure S7). The CT transition and second band are indicative of a weaker ligand field consistent with the ligand set of the MBSA.[38,46] While a d−d band with λ_{max} at 650 and 725 nm is observed upon addition of 1 and 2 equivalents of Cu(II), respectively, to apo-C-peptide (Figure 5B, Tables 4 and 5), the extinction coefficient of these peaks are significantly lower than that of the Cu(II)-BSA sites. We thus used the Cu(II)-BSA signatures as a point of comparison to assess the C-peptide/BSA/Cu(II) complexes.

Table 4. Maximum Absorbance Values of the UV−Vis Spectra with the Addition of One Equivalence of Cu(II) (Dashed Line)

one equivalence Cu(II) (dashed)		
samples	Abs_{max} (nm)	
Cu(II)−C-peptide	---	650
Cu(II)-BSA	---	540
C-peptide +1:1 Cu(II)-BSA	---	545
1:1 Cu(II)−C-peptide + BSA	360	525

Table 5. Maximum Absorbance Values of the UV−Vis Spectra with the Addition of Two Equivalences of Cu(II) (Solid Line)

two equivalences Cu(II) (solid)			
samples	Abs_{max} (nm)		
Cu(II)−C-peptide	—	—	725
Cu(II)-BSA	385	555	680
C-peptide + 2:1 Cu(II)-BSA	388	556	678
2:1 Cu(II)−C-peptide + BSA	375	530	690

Spectral traces of the C-peptide/BSA/Cu(II) complexes were subtracted from the summation of the apo-C-peptide and apo-BSA spectra to focus the analysis on the Cu(II) d−d bands (Figure S8). Relative to the spectra of metalated BSA, the C-peptide + Cu(II)-BSA complex at one equivalent Cu(II) shows a red shift in the λ_{max} from 540 to 545 nm (Figure 5B, Table 4), indicative of a weaker field ligand environment compared to 1:1 Cu(II)-BSA. However, at two equivalents Cu(II), the C-peptide + Cu(II)-BSA spectrum closely overlaps with that of the 2:1 Cu(II)-BSA spectra with minimal shifts in λ_{max} at 388, 556, and 678 nm (Figure 5A,B, Table 5). In contrast, the Cu(II)−C-peptide + BSA complex at one equivalent of Cu(II) blue-shifts the λ_{max} to 525 nm relative to the 540-nm peak of 1:1 Cu(II)-BSA and interestingly produces a CT band at 360 nm (Figure 5A, Table 4), suggesting a stronger field ligand set compared to 1:1 Cu(II)-BSA. At two equivalents of Cu(II), the spectrum of the Cu(II)−C-peptide + BSA complex yield blue-shifted absorption maxima at 375 and 530 nm relative to the 385 nm and 555 nm bands of 2:1 Cu(II)-BSA, while a 690 nm peak is observed red-shifted from the 680 nm band of Cu(II)-BSA (Figure 5A and Table 5). To ensure that the C-peptide/BSA/Cu(II) traces are not merely the additive spectra of the species in solution, we summed the independent traces of C-peptide, BSA, or their Cu(II) complexes accordingly to mimic the sample preparation conditions of each scheme (Figure S9, Tables S1 and S2). The addition spectra show marked differences from the experimental spectra, both in terms of overall spectral profile and absorption maxima, suggesting that the C-peptide + Cu(II)-BSA and Cu(II)−C-peptide + BSA preparations do indeed result in new species as evidenced by the alterations in their d−d band positions.

https://doi.org/10.1021/jacs.3c04599
J. Am. Chem. Soc. 2023, 145, 16726−16738

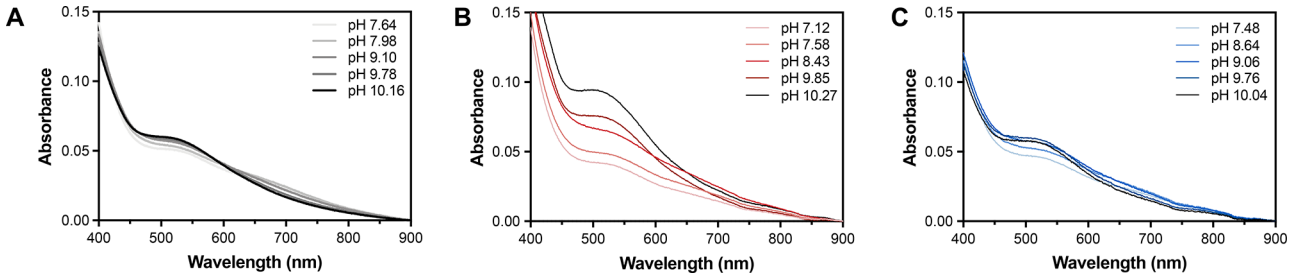

Figure 6. Electronic absorption spectra of pH titrations at two equivalents Cu(II). Samples were prepared in 10 mM phosphate buffer with 300 μM of C-peptide and/or BSA with 300 μM (1 equivalent) $CuCl_2$. (A) Cu(II)-BSA, (B) C-peptide + Cu(II)-BSA, and (C) Cu(II)−C-peptide + BSA were prepped in neutral pH conditions, then titrated with 15 mM NaOH solution until basic pH conditions are reached. Selected traces are displayed in each figure to show shifts in absorbance peaks with regards to pH dependence. The differences in the pH behavior of the three species suggest that the order of addition leads to either differences in coordinating ligands or in global conformation.

We further characterized the chemical differences between the C-peptide + Cu(II)-BSA and the Cu(II)−C-peptide + BSA complexes, by assessing their pH stability via their d−d bands. The complexes were prepared at neutral pH than titrated with NaOH to raise the pH of the solutions (Figure 6). Upon an increase in pH only the C-peptide + Cu(II)-BSA complex exhibits a significant change in absorption intensity at the d−d region (Figure 6B). This change at 535 nm corresponds to a deprotonation of the backbone amide nitrogens at the NTS BSA site.[19,54,55] Conversely, upon an increase in pH, the Cu(II)−C-peptide + BSA complex does not yield significant changes in absorption (Figure 6C), providing further evidence that the two C-peptide/BSA/Cu(II) species are distinct.

While the pH-dependent behaviors of the two species could point to differences in coordinating ligands, they may alternatively arise from global conformational differences that affect the pH stability of the Cu(II) sites on albumin. To untangle these contributions, we probed the coordination environment and geometry around the Cu(II) center of the complexes with electron paramagnetic resonance (EPR) spectroscopy. Previous work has shown that the NTS of serum albumin is a square-planar coordination site of four nitrogen ligands which include the N-terminus, two backbone amide nitrogen atoms, and one His residue (Figure S1A).[56] The MBSA contains two nitrogen ligands, both from His residues, one oxygen ligand from an Asn residue and a second oxygen ligand from an Asp residue to make a tetrahedral 2N2O site (Figure S1A).[57]

We compared the Cu(II) coordination environment of the C-peptide/BSA/Cu(II) complexes to that of BSA alone. At X-band frequency (9.39 GHz), the EPR spectra of the two complexes at one equivalent Cu(II) are identical to that of Cu(II)-BSA (Figure S10); all species exhibit an axial signal with hyperfine interactions to the Cu(II) nucleus. Simulation was achieved using $g_{\|}$ = 2.183 and $A_{\|}$ = 601 MHz. This result indicates no change in coordination modes at the NTS of BSA in either complex. The parameters from the Cu(II)−C-peptide EPR spectrum at X-band frequency did not overlap with those of either complexes, confirming that Cu(II)−C-peptide species were not present or detected (Figure S11 and Table S3).[15] Upon addition of two equivalents Cu(II), a second paramagnetic copper species with $g_{\|}$ = 2.27, $g_{\perp}$ = 2.055 and $A_{\|}$ = 545 MHz was detected in all samples (Figure 7A, Table 6, Figure S12A and S12B). For Cu(II)-BSA, this is consistent with metalation of the MBSA as previously observed.[58] Importantly, no change in EPR spectra were observed upon the addition of C-peptide, which suggests similarities in the coordination environment around the Cu(II) center to the MBSA in Cu(II)-BSA.

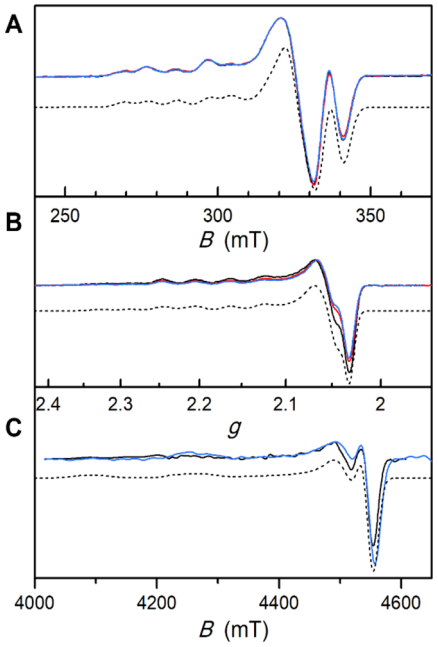

Figure 7. Determination of coordination modes using EPR at X-, Q-, and D-bands at two equivalents of Cu(II). (A) X-band continuous-wave EPR spectra of Cu(II)-BSA (black), C-peptide + Cu(II)-BSA (red), and Cu(II)−C-peptide + BSA (blue) at two equivalents of Cu(II) concentration measured at 20 K. (B) Q-band field-sweep echo-detected EPR spectra of Cu(II)-BSA, C-peptide + Cu(II)-BSA, and Cu(II)−C-peptide + BSA measured at 25 K. The spectra were taken at microwave frequencies 34.296, 33.958, and 34.293 GHz, respectively, and were overlaid onto the common *g*-factor abscissa. The spectra were pseudo-modulated at 3 mT. (C) D-band field-sweep echo-detected EPR spectra of Cu(II)-BSA and Cu(II)−C-peptide + BSA at 10 and 13 K, respectively. The spectra were pseudo-modulated at 20 mT. Black dashed lines are simulations of the data using the parameters given in Table 6, which are labeled in Figure S9.

To discern subtle differences, the samples were investigated at higher frequencies. At Q-band frequency, the EPR spectra of the C-peptide/BSA/Cu(II) complexes remain similar to that of Cu(II)-BSA (Figures 7B, S12A and S12B). We further investigated Cu(II)-BSA and the Cu(II)−C-peptide + BSA complex at D-band frequency (130 GHz) (Figures 7C and S12B) due to the differences observed in the UV−Vis absorption spectra (Figure 5A). To our knowledge, this is the first time that the Cu(II)-BSA complex has been

https://doi.org/10.1021/jacs.3c04599
J. Am. Chem. Soc. 2023, 145, 16726−16738

Table 6. EPR Simulation Parameters for Cu(II)-BSA, C-peptide + Cu(II)-BSA, and Cu(II)−C-peptide + BSA

	NTS site	MBSA site
$g_{\parallel}$	2.183	2.270
$g_{\perp}$	2.0418	2.055
$A_{\parallel}$ (MHz)	601	545
$A_{\perp}$ (MHz)	80	0
linewidth (X-band, mT)	5	5
linewidth (Q-band, mT)	6	11
linewidth (D-band, mT)	15	35
relative ratio	0.5	0.5

investigated via high-field EPR. The resulting spectra allow a precise determination of $g_{\perp}$ = 2.042 for the NTS and 2.055 for the MBSA. The simultaneous simulation of all EPR spectra yield $g_{\parallel}$ and $A_{\parallel}$ values (Table 6) indicative of a neutral 4 N coordination for the first site, and a neutral 2N2O coordination for the second site,[59] which is in agreement with the assignment of the NTS and MBSA, respectively. These parameters do not change significantly in either C-peptide/BSA/Cu(II) complex, suggesting conserved coordination environments around the Cu(II) centers compared to the equimolar Cu(II)-BSA species.

The EPR and electronic absorption data together suggest that while the Cu(II) species in both C-peptide/BSA/Cu(II) complexes are distinct from metalated BSA, their metal coordination environments exhibit similar geometries and atom identities. Thus, to understand what leads to the slight shifts in the absorption maxima of the UV−Vis spectra of the C-peptide/BSA/Cu(II) complexes relative to Cu(II)/BSA alone, we applied TDDFT to predict the visible spectra of hypothesized binding modes.[60] Geometry optimization and TDDFT calculations were constructed for both Cu(II) binding sites of BSA and Cu(II)−C-peptide (Figure S13A,B and Tables S4−S6). The TDDFT calculations (Table S7) reveal that displacement of Asp249 at the MBSA of BSA (Figure 8A) by Asp4 of C-peptide (Figure 8B) results in a modest blue shift in the λ_{max} from 721 to 688 nm (Figure 8C), which resembles the observed experimental shift in the UV−Vis spectrum of the 2:1 C-peptide + Cu(II)-BSA complex (Figure 8B). Modifications of TDDFT calculations with other residues of the C-peptide terminus yield various models and electronics that do not support this experimental shift. Rather, the subtle change in the λ_{max} value may be attributed to a shift in sterics in the outer coordination sphere[61,62] as Asp4 of C-peptide coordinates.

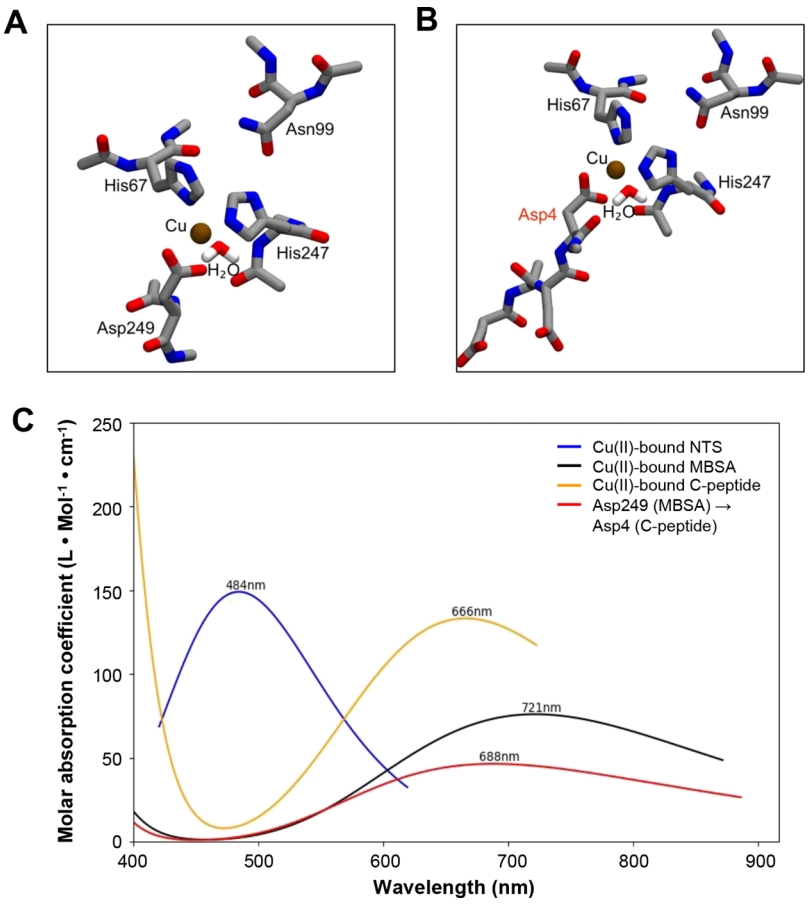

Figure 8. Modeled copper coordination ligand sets between C-peptide and BSA using TDDFT calculations. (A) Established structure of the copper-binding MBSA in BSA, where His67, His247, Asp249, and H_2O are coordinated to the copper center following a tetrahedral 2N2O site, and Asn99 is displaced. (B) Hypothetical coordination model of the displacement of Asp249 from the MBSA to Asp4 of C-peptide. (C) Resulting TDDFT calculations of predicted wavelengths based on optimized geometries of the Cu(II)-bound NTS (blue) and the Cu(II)-bound MBSA (black) of BSA, as well as Cu(II)-bound C-peptide (orange). The displacement of Asp249 in the MBSA of BSA to Asp4 of C-peptide results in a blue-shifted λ_{max} at 688 nm (red) from the MBSA trace at 721 nm (black).

https://doi.org/10.1021/jacs.3c04599
J. Am. Chem. Soc. 2023, 145, 16726−16738

Importantly, this hypothesis of this steric shift in the outer sphere is also consistent with minimal perturbations in the primary coordination sphere observed by EPR. DFT calculations of EPR parameters using the PBE0 functional[54] give $g_{||}$ = 2.237 for the Cu(II) center in the MBSA, and $g_{||}$ = 2.233 for the Cu(II) ternary complex with the MBSA and C-peptide Asp4 residue (Table S8). Although there is a slight discrepancy in the $g_{||}$ value from the experimental value, the difference in $g_{||}$ of the Cu site with and without C-peptide is minimally small, in congruence with experimental observations. Calculation of the $A_{||}$ parameter performed with the B3LYP functional[63] gives $|A_{||}|$ = 546 and 549 MHz for Cu-BSA and C-peptide/BSA/Cu(II) models, respectively, in excellent agreement with experimental values (Table S8). Altogether, the agreement between TDDFT calculations and the experimental UV−Vis and EPR spectra supports the role of Cu(II) in bridging the interaction between C-peptide and BSA at the MBS via retention of a coordinating Asp from C-peptide and replacement of the remaining Cu(II) ligand set of C-peptide with the MBSA ligands of BSA.

The TDDFT calculations lend insight into the comparable coordination geometry of the C-peptide + Cu(II)-BSA complex and resulting steric shift due to the Asp residue swap. Conversely, the red shift to λ_{max} at 690 nm and rise in intensity of the CT band observed in the experimental spectrum off the Cu(II)−C-peptide + BSA Complex (Figure 5A), could not be emulated by the predicted spectra of the model structures. We thus considered whether the Cu(II)−C-peptide + BSA complex involves a different Cu(II)-binding region on C-peptide. In our previous studies, we made an intriguing finding that mutating or truncating C-peptide to perturb the putative Glu3 and Asp4 binding sites does not eradicate Cu(II) binding but reshuffles coordination to different sites on the peptide, as determined by regional signal loss in the NMR spectra.[15] While addition of Cu(II) to the wild-type peptide yields paramagnetic signal loss at the Glu3 and Asp4 side chain protons at the N-terminal region, replacing these residues with Ala (the E3AD4A mutant peptide) redirects the signal loss and suggests Cu(II) binding to other regions of the peptide, including the Gln9-Leu12 region, which contains a Glu residue at position 11, and the C-terminal region, which contains a Glu residue at position 27. A C-terminal truncate containing the Leu24-Gln31 residues (C-term) shows signal loss at Glu27, implicating the residue in Cu(II) binding. Interestingly, a N-terminal truncate containing Glu1−Gly13 (N-term) shows signal loss or broadening not only at the Glu3/Asp4 side chains, but also at the Glu1 and Glu11 residues. Despite the differences in binding regions, the mutant and truncates exhibit similar coordination environments to the wild type (1NO3 square-planar geometry) as indicated by similarities in the EPR spectra, d−d band positions, and thermodynamic parameters.

These previous studies suggest that Cu(II) can bind to C-peptide on different sites beyond the Glu3/Asp4 residues with similar coordination environments. To determine whether such a reshuffled binding may occur with the Cu(II)−C-peptide + BSA complexes, we compared the electronic absorption spectra of the Cu(II)−C-peptide + BSA complex (at 2 equivalence Cu(II)) to similar preparations but with the E3AD4A, C-term, and N-term peptides (Figure 9). We observed a strong resemblance in the spectra of Cu(II)−N-term + BSA, including the red-shift in the d−d band, relative to Cu(II)-BSA as well as the increased intensity of a CT band.

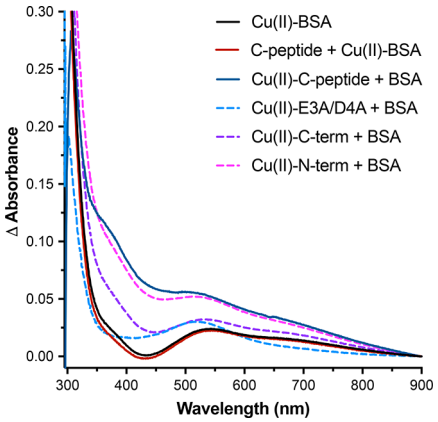

Figure 9. Comparison of the UV−Visible spectra between Cu(II)−C-peptide + BSA (solid blue) and Cu(II)-peptide + BSA preparations with varying C-peptide mutants that were previously reported to have reshuffled Cu(II) binding: a mutant wherein the putative Glu3 and Asp4 Cu(II) binding residues are mutated to Ala (E3A/D4A peptide, dashed blue), a C-terminal truncate containing the Leu24-Gln31 residues (C-term, dashed purple), and an N-terminal truncate containing Glu1−Gly13 residues (N-term, dashed pink). Cu(II)-BSA (solid black) and C-peptide + Cu(II)-BSA (solid red) are provided for reference. Samples were prepared in 10 mM phosphate buffer with 300 μM of peptide and/or BSA. Spectra represent preparations with 2 equivalents (600 μM) of Cu(II) to both C-peptide and BSA (which are equimolar when both are present). Cu(II)−C-peptide + BSA shows a strong resemblance to the spectra of Cu(II)-N-term + BSA, suggesting similarities in their global conformations.

These data support the notion that addition of BSA to Cu(II)−C-peptide may reshuffle the binding of Cu(II) toward an interaction similar to that which occurs on the N-term peptide. We thus propose that the divergent structure and behavior of the ternary complexes that arise from order of addition result from differences in orientation of C-peptide and albumin around the Cu(II) center.

CONCLUSIONS

In this work, we present evidence for ternary complexes involving C-peptide, Cu(II), and albumin. The complexes require Cu(II) to form and do not form either in the absence of Cu(II) or with the addition Zn(II) addition. The structure of albumin is altered upon incubation with Cu(II) and C-peptide, and distinct species are formed based on the order of addition. While the Cu(II) binding environments show similarities to a Cu(II)-BSA complex, spectroscopic and computational work suggest differences in ligand identities and global structure of the biomolecules. The C-peptide + Cu(II)-BSA complex corresponds to a binding scenario wherein the Asp249 of the MBSA in BSA is exchanged with the Asp4 of C-peptide. The Cu(II)−C-peptide + BSA complex is spectroscopically distinct from C-peptide + Cu(II)-BSA and Cu(II)-BSA alone. While the exact ligand identities require further investigation, our findings suggest a level of binding precision within albumin that is influenced by the surrounding ligands of the added Cu(II) species.

These ternary complexes exhibit biological activity that differ from metalated C-peptide or BSA. Both C-peptide/BSA/Cu(II) species impact biochemical activity of the bound Cu(II) to a similar degree, exhibiting higher redox protection on Cu(II) than either C-peptide or BSA. However, the

https://doi.org/10.1021/jacs.3c04599
J. Am. Chem. Soc. 2023, 145, 16726−16738

complexes differ in their effects on cellular behavior: while the C-peptide + Cu(II)-BSA complex shows a reduction in C-peptide internalization similar to the addition of Cu(II) to the peptide in the absence of BSA, the Cu(II)−C-peptide + BSA complex has the opposite behavior, enhancing C-peptide internalization over that of C-peptide alone. This observation may support the notion that a cognate receptor recognizes the albumin-associated C-peptide rather than the unassociated peptide[13,14] and that Cu(II) may be an important factor in stabilizing this complex. Taken together, consideration of the ternary complexes may be essential to untangling C-peptide's mechanism of action.

The two C-peptide/BSA/Cu(II) complexes may also bear clinical relevance to C-peptide measurements by standard bioassays. As C-peptide is used as a proxy for assessing insulin secretory health, these assays are most frequently conducted in patients with insulin-associated dysfunctions such as diabetes.[31,32] Of note, many of these disorders are associated with elevated serum copper levels.[64−66] Independently of copper levels, shifts in albumin levels have been linked to diabetes risk and progression.[67−69] As both complexes significantly increased the observed C-peptide levels in comparison to C-peptide alone, our data point to the importance of considering C-peptide measurements alongside copper and albumin levels. While further investigations are required to determine if the C-peptide/BSA/Cu(II) species form in vivo, the concomitant changes in copper, albumin, and C-peptide in diabetic states may point to the value of such ternary complexes as biomarkers. Beyond C-peptide, this work offers additional opportunities to investigate the impact of plasma proteins on metal-binding peptides in extracellular signaling, further highlighting a need for studies on the biological and clinical implications of regulatory partners associated with bioactive peptides.

■ ASSOCIATED CONTENT

Supporting Information

The Supporting Information is available free of charge at https://pubs.acs.org/doi/10.1021/jacs.3c04599.

Detailed procedures and supporting experimental data figures and tables (PDF)

■ AUTHOR INFORMATION

Corresponding Author

Marie C. Heffern − *Department of Chemistry, University of California, Davis, California 95616, United States;* orcid.org/0000-0001-7501-2741; Email: mcheffern@ucdavis.edu

Authors

Jessica A. San Juan − *Department of Chemistry, University of California, Davis, California 95616, United States;* orcid.org/0000-0002-7657-3716

Khetpakorn Chakarawet − *Department of Chemistry, University of California, Davis, California 95616, United States;* Present Address: Department of Chemistry, Faculty of Science, Mahidol University, Bangkok 10400 Thailand; orcid.org/0000-0001-5905-3578

Zhecheng He − *Department of Chemistry, University of California, Davis, California 95616, United States*

Rebeca L. Fernandez − *Department of Chemistry, University of California, Davis, California 95616, United States;* orcid.org/0000-0003-1459-9731

Michael J. Stevenson − *Department of Chemistry, University of San Francisco, San Francisco, California 94117, United States;* orcid.org/0000-0002-0064-0230

Nathaniel H. O. Harder − *Department of Chemistry, University of California, Davis, California 95616, United States*

Samuel E. Janisse − *Department of Chemistry, University of California, Davis, California 95616, United States*

Lee-Ping Wang − *Department of Chemistry, University of California, Davis, California 95616, United States;* orcid.org/0000-0003-3072-9946

R. David Britt − *Department of Chemistry, University of California, Davis, California 95616, United States;* orcid.org/0000-0003-0889-8436

Complete contact information is available at: https://pubs.acs.org/10.1021/jacs.3c04599

Notes

The authors declare no competing financial interest.

■ ACKNOWLEDGMENTS

This work was supported by the National Institutes of Health (NIH MIRA 5R35GM133684 and P30DK098722 to M.C.H. and the NIH MIRA 535GM133684-04S1 supplement to support R.L.F.) and the National Science Foundation (NSF CAREER 2048265 to M.C.H.). We also thank the Hartwell Foundation for their generous support for M.C.H. as a Hartwell Individual Biomedical Investigator, as well as the UC Davis CAMPOS Program and the University of California's Presidential Postdoctoral Fellowship for their support of M.C.H. as a CAMPOS Faculty Fellow and former UC President's Postdoctoral Fellow, respectively. EPR spectroscopic studies were funded by the National Institutes of Health (NIH R35GM126961 to R.D.B.). Computational work was funded by the National Institutes of Health (NIH R01AI130684 to L.P.W.). We thank Dr. Lizhi Tao and Dr. Richard Sayler for helpful discussions regarding EPR spectroscopy. We also like to thank Ryan L. Neil and Quang D. Pham for help with the C-peptide and TAMRA-C-peptide synthesis and all members of the Heffern lab for valuable discussions.

■ REFERENCES

(1) Fricker, L. D.; Devi, L. A. Orphan Neuropeptides and Receptors: Novel Therapeutic Targets. *Pharmacol. Ther.* **2018**, *185*, 26.

(2) Fosgerau, K.; Hoffmann, T. Peptide Therapeutics: Current Status and Future Directions. *Drug Discovery Today* **2015**, *20*, 122−128.

(3) Saltiel, A. R.; Kahn, C. R. Insulin Signalling and the Regulation of Glucose and Lipid Metabolism. *Nature* **2001**, *414*, 799−806.

(4) Manning, M.; Stoev, S.; Chini, B.; Durroux, T.; Mouillac, B.; Guillon, G. Peptide and Non-Peptide Agonists and Antagonists for the Vasopressin and Oxytocin V1a, V1b, V2 and OT Receptors: Research Tools and Potential Therapeutic Agents. *Prog. Brain Res.* **2008**, *170*, 473−512.

(5) Mirabeau, O.; Perlas, E.; Severini, C.; Audero, E.; Gascuel, O.; Possenti, R.; Birney, E.; Rosenthal, N.; Gross, C. Identification of Novel Peptide Hormones in the Human Proteome by Hidden Markov Model Screening. *Genome Res.* **2007**, *17*, 320.

(6) Wahren, J.; Ekberg, K.; Jörnvall, H. C-Peptide Is a Bioactive Peptide. In *Diabetologia*; Springer, 2007, pp 503−509.

(7) Marques, R. G.; Fontaine, M. J.; Rogers, J. C-Peptide: Much More than a Byproduct of Insulin Biosynthesis. *Pancreas* **2004**, *29*, 231−238.
(8) Pinger, C. W.; Entwistle, K. E.; Bell, T. M.; Liu, Y.; Spence, D. M. C-Peptide Replacement Therapy in Type 1 Diabetes: Are We in the Trough of Disillusionment? *Mol. Biosyst.* **2017**, *13*, 1432−1437.
(9) Washburn, R. L.; Mueller, K.; Kaur, G.; Moreno, T.; Moustaid-moussa, N.; Ramalingam, L.; Dufour, J. M. C-peptide as a Therapy for Type 1 Diabetes Mellitus. *Biomedicines* **2021**, *9*, 270.
(10) Lindfors, L.; Sundström, L.; Fröderberg Roth, L.; Meuller, J.; Andersson, S.; Kihlberg, J. Is GPR146 Really the Receptor for Proinsulin C-Peptide? *Bioorg. Med. Chem. Lett.* **2020**, *30*, No. 127208.
(11) Yosten, G. L. C.; Kolar, G. R.; Redlinger, L. J.; Samson, W. K. Evidence for an Interaction between Proinsulin C-Peptide and GPR146. *J. Endocrinol.* **2013**, *218*, B1.
(12) Rossiter, J. L.; Redlinger, L. J.; Kolar, G. R.; Samson, W. K.; Yosten, G. L. C. The Actions of C-Peptide in HEK293 Cells Are Dependent upon Insulin and Extracellular Glucose Concentrations. *Peptides* **2022**, *150*, No. 170718.
(13) Liu, Y.; Chen, C.; Summers, S.; Medawala, W.; Spence, D. M. C-Peptide and Zinc Delivery to Erythrocytes Requires the Presence of Albumin: Implications in Diabetes Explored with a 3D-Printed Fluidic Device. *Integr. Biol.* **2015**, *7*, 534−543.
(14) Geiger, M.; Janes, T.; Keshavarz, H.; Summers, S.; Pinger, C.; Fletcher, D.; Zinn, K.; Tennakoon, M.; Karunarathne, A.; Spence, D. A C-Peptide Complex with Albumin and Zn2+ Increases Measurable GLUT1 Levels in Membranes of Human Red Blood Cells. *Sci. Rep.* **2020**, *10*, 17493.
(15) Stevenson, M. J.; Janisse, S. E.; Tao, L.; Neil, R. L.; Pham, Q. D.; Britt, R. D.; Heffern, M. C. Elucidation of a Copper Binding Site in Proinsulin C-Peptide and Its Implications for Metal-Modulated Activity. *Inorg. Chem.* **2020**, *59*, 9339−9349.
(16) Stevenson, M. J.; Farran, I. C.; Uyeda, K. S.; San Juan, J. A.; Heffern, M. C. Analysis of Metal Effects on C-Peptide Structure and Internalization. *ChemBioChem* **2019**, *20*, 2447−2453.
(17) Kleine, B.; Rossmanith, W. G. *Hormones and the Endocrine System*; Springer, 2016, DOI: 10.1007/978-3-319-15060-4.
(18) Zolla, L. Proteomics Studies Reveal Important Information on Small Molecule Therapeutics: A Case Study on Plasma Proteins. *Drug Discovery Today* **2008**, *13*, 1042.
(19) Bal, W.; Sokołowska, M.; Kurowska, E.; Faller, P. Binding of Transition Metal Ions to Albumin: Sites, Affinities and Rates. *Biochim. Biophys. Acta Gen. Subj. BBA−Gen. Subjects* **2013**, 5444−5455.
(20) Stefaniak, E.; Płonka, D.; Drew, S. C.; Bossak-Ahmad, K.; Haas, K. L.; Pushie, M. J.; Faller, P.; Wezynfeld, N. E.; Bal, W. The N-Terminal 14-Mer Model Peptide of Human Ctr1 Can Collect Cu(Ii) from Albumin. Implications for Copper Uptake by Ctr1. *Metallomics* **2018**, *10*, 1723−1727.
(21) Krause-Heuer, A. M.; Price, W. S.; Aldrich-Wright, J. R. Spectroscopic Investigations on the Interactions of Potent Platinum-(II) Anticancer Agents with Bovine Serum Albumin. *J. Chem. Biol.* **2012**, *5*, 105.
(22) Shahabadi, N.; Hadidi, S. Mechanistic and Conformational Studies on the Interaction of a Platinum(II) Complex Containing an Antiepileptic Drug, Levetiracetam, with Bovine Serum Albumin by Optical Spectroscopic Techniques in Aqueous Solution. *Appl. Biochem. Biotechnol.* **2015**, *175*, 1843−1857.
(23) Choi, T. S.; Lee, H. J.; Han, J. Y.; Lim, M. H.; Kim, H. I. Molecular Insights into Human Serum Albumin as a Receptor of Amyloid-β in the Extracellular Region. *J. Am. Chem. Soc.* **2017**, *139*, 15437−15445.
(24) Rózga, M.; Bal, W. The Cu(II)/Abeta/Human Serum Albumin Model of Control Mechanism for Copper-Related Amyloid Neurotoxicity. *Chem. Res. Toxicol.* **2010**, *23*, 298−308.
(25) Perrone, L.; Mothes, E.; Vignes, M.; Mockel, A.; Figueroa, C.; Miquel, M. C.; Maddelein, M. L.; Faller, P. Copper Transfer from Cu-Abeta to Human Serum Albumin Inhibits Aggregation, Radical Production and Reduces Abeta Toxicity. *ChemBioChem* **2010**, *11*, 110−118.
(26) Lu, N.; Yang, Q.; Li, J.; Tian, R.; Peng, Y. Y. Inhibitory Effect of Human Serum Albumin on Cu-Induced Aβ(40) Aggregation and Toxicity. *Eur. J. Pharmacol.* **2015**, *767*, 160−164.
(27) Han, J.; Yoon, J.; Shin, J.; Nam, E.; Qian, T.; Li, Y.; Park, K.; Lee, S. H.; Lim, M. H. Conformational and Functional Changes of the Native Neuropeptide Somatostatin Occur in the Presence of Copper and Amyloid-β. *Nat. Chem.* **2022**, *14*, 1021.
(28) Bossak-Ahmad, K.; Bal, W.; Frączyk, T.; Drew, S. C. Ternary Cu^{2+} Complexes of Human Serum Albumin and Glycyl-L-Histidyl-L-Lysine. *Inorg. Chem.* **2021**, *60*, 16927−16931.
(29) Meyer, J. A.; Froelich, J. M.; Reid, G. E.; Karunarathne, W. K. A.; Spence, D. M. Metal-Activated C-Peptide Facilitates Glucose Clearance and the Release of a Nitric Oxide Stimulus via the GLUT1 Transporter. *Diabetologia* **2008**, *51*, 175−182.
(30) Meyer, J. A.; Subasinghe, W.; Sima, A. A. F.; Keltner, Z.; Reid, G. E.; Daleke, D.; Spence, D. M. Zinc-Activated C-Peptide Resistance to the Type 2 Diabetic Erythrocyte Is Associated with Hyperglycemia-Induced Phosphatidylserine Externalization and Reversed by Metformin. *Mol. BioSyst.* **2009**, *5*, 1157−1162.
(31) Jones, A. G.; Hattersley, A. T. The Clinical Utility of C-Peptide Measurement in the Care of Patients with Diabetes. *Diabet. Med.* **2013**, *30*, 803−817.
(32) Leighton, E.; Sainsbury, C. A.; Jones, G. C. A Practical Review of C-Peptide Testing in Diabetes. *Diabetes Ther.* **2017**, *8*, 475−487.
(33) Faber, O. K.; Hagen, C.; Binder, C.; Markussen, J.; Naithani, V. K.; Blix, P. M.; Kuzuya, H.; Horwitz, D. L.; Rubenstein, A. H.; Rossing, N. Kinetics of Human Connecting Peptide in Normal and Diabetic Subjects. *J. Clin. Invest.* **1978**, *62*, 197−203.
(34) Lakowicz, J. R. *Principles of Fluorescence Spectroscopy*, 3rd ed.; Lakowicz, J. R., Eds.; 2006.
(35) Berney, C.; Danuser, G. FRET or No FRET: A Quantitative Comparison. *Biophys. J.* **2003**, *84*, 3992.
(36) Foley, T. L.; Burkart, M. D. A Homogeneous Resonance Energy Transfer Assay for Phosphopantetheinyl Transferase. *Anal. Biochem.* **2009**, *394*, 39−47.
(37) Liu, Y.; Chen, M.; Song, L. Comparing the Effects of Fe(III) and Cu(II) on the Binding Affinity of Erlotinib to Bovine Serum Albumin Using Spectroscopic Methods. *J. Lumin.* **2013**, *134*, 515−523.
(38) Zhang, Y.; Wilcox, D. E. Thermodynamic and Spectroscopic Study of Cu(II) and Ni(II) Binding to Bovine Serum Albumin. *J. Biol. Inorg. Chem.* **2002**, *7*, 327−337.
(39) Masuoka, J.; Saltman, P. Zinc(II) and Copper(II) Binding to Serum Albumin: A Comparative Study of Dog, Bovine, and Human Albumin. *J. Biol. Chem.* **1994**, *269*, 25557−25561.
(40) Greenfield, N. J. Using Circular Dichroism Collected as a Function of Temperature to Determine the Thermodynamics of Protein Unfolding and Binding Interactions. *Nat. Protoc.* **2006**, *1*, 2527−2535.
(41) Kelly, S. M.; Jess, T. J.; Price, N. C. How to Study Proteins by Circular Dichroism. *Biochim. Biophys. Acta, Proteins Proteomics* **2005**, *1751*, 119−139.
(42) Buddanavar, A. T.; Nandibewoor, S. T. Multi-Spectroscopic Characterization of Bovine Serum Albumin upon Interaction with Atomoxetine. *J. Pharm. Anal.* **2017**, *7*, 148−155.
(43) Varlan, A.; Hillebrand, M. Bovine and Human Serum Albumin Interactions with 3-Carboxyphenoxathiin Studied by Fluorescence and Circular Dichroism Spectroscopy. *Molecules* **2010**, *15*, 3905−3919.
(44) Shahabadi, N.; Hadidi, S.; Kalar, Z. M. Biophysical Studies on the Interaction of Platinum(II) Complex Containing Antiviral Drug Ribavirin with Human Serum Albumin. *J. Photochem. Photobiol., B* **2016**, *160*, 376−382.
(45) Jing, M.; Liu, R.; Yan, W.; Tan, X.; Chen, Y. Investigations on the Effects of Cu^{2+} on the Structure and Function of Human Serum Albumin. *Luminescence* **2016**, *31*, 557−564.
(46) Peters, T.; Blumenstock, F. A. Copper-Binding Properties of Bovine Serum Albumin and Its Amino-Terminal Peptide Fragment. *J. Biol. Chem.* **1967**, *242*, 1574−1578.

(47) Hu, X.; Zhang, Q.; Wang, W.; Yuan, Z.; Zhu, X.; Chen, B.; Chen, X. Tripeptide GGH as the Inhibitor of Copper-Amyloid-β-Mediated Redox Reaction and Toxicity. *ACS Chem. Neurosci.* **2016**, *7*, 1255−1263.
(48) Meloni, G.; Faller, P.; Vašák, M. Redox Silencing of Copper in Metal-Linked Neurodegenerative Disorders: Reaction of Zn_7 metallothionein-3 with Cu^{2+} Ions. *J. Biol. Chem.* **2007**, *282*, 16068−16078.
(49) Lindahl, E.; Nyman, U.; Melles, E.; Sigmundsson, K.; Ståhlberg, M.; Wahren, J.; Öbrink, B.; Shafqat, J.; Joseph, B.; Jörnvall, H. Cellular Internalization of Proinsulin C-Peptide. *Cell. Mol. Life Sci.* **2007**, *64*, 479−486.
(50) Francis, G. L. Albumin and mammalian cell culture: implications for biotechnology applications. *Cytotechnology* **2010**, *62*, 1−16.
(51) Unnerståle, S.; Mäler, L. PH-Dependent Interaction between C-Peptide and Phospholipid Bicelles. *J. Biophys.* **2012**, *2012*, No. 185907.
(52) Luppi, P.; Geng, X.; Cifarelli, V.; Drain, P.; Trucco, M. C-Peptide Is Internalised in Human Endothelial and Vascular Smooth Muscle Cells via Early Endosomes. *Diabetologia* **2009**, *52*, 2218−2228.
(53) Frei, E. Albumin Binding Ligands and Albumin Conjugate Uptake by Cancer Cells. *Diabetol. Metab. Syndr.* **2011**, *3*, 11.
(54) Neupane, K. P.; Aldous, A. R.; Kritzer, J. A. Metal-binding and redox properties of substituted linear and cyclic ATCUN motifs. *J. Inorg. Biochem.* **2014**, *139*, 65−76.
(55) Sóvágó, I.; Osz, K. Metal ion selectivity of oligopeptides. *Dalton Trans.* **2006**, *32*, 3841−3854.
(56) Kozlowski, H.; Bal, W.; Dyba, M.; Kowalik-Jankowska, T. Specific Structure-Stability Relations in Metallopeptides. *Coord. Chem. Rev.* **1999**, *184*, 319−346.
(57) Handing, K. B.; Shabalin, I. G.; Kassaar, O.; Khazaipoul, S.; Blindauer, C. A.; Stewart, A. J.; Chruszcz, M.; Minor, W. Circulatory Zinc Transport Is Controlled by Distinct Interdomain Sites on Mammalian Albumins. *Chem. Sci.* **2016**, *7*, 6635−6648.
(58) Pandeya, K.; Patel, R. X-Band Electron Paramagnetic Resonance Spectra of Bovine Serum Albumin-Copper (II) and Bovine Serum Albumin-Copper (II)-Aminoacid Systems. *Indian J. Biochem. Biophys.* **1992**, *29*, 245−250.
(59) Peisach, J.; Blumberg, W. E. Structural Implications Derived from the Analysis of Electron Paramagnetic Resonance Spectra of Natural and Artificial Copper Proteins. *Arch. Biochem. Biophys.* **1974**, *165*, 691−708.
(60) Sciortino, G.; Maréchal, J. D.; Fábián, I.; Lihi, N.; Garribba, E. Quantitative Prediction of Electronic Absorption Spectra of Copper-(II)−Bioligand Systems: Validation and Applications. *J. Inorg. Biochem.* **2020**, *204*, No. 110953.
(61) Warren, J. J.; Lancaster, K. M.; Richards, J. H.; Gray, H. B. Inner- and Outer-Sphere Metal Coordination in Blue Copper Proteins. *J. Inorg. Biochem.* **2012**, *115*, 119−126.
(62) Ruckthong, L.; Stuckey, J. A.; Pecoraro, V. L. How Outer Coordination Sphere Modifications Can Impact Metal Structures in Proteins: A Crystallographic Evaluation. *Chem. − A Eur. J.* **2019**, *25*, 6773−6787.
(63) Sciortino, G.; Lubinu, G.; Maréchal, J. D.; Garribba, E. DFT Protocol for EPR Prediction of Paramagnetic Cu(II) Complexes and Application to Protein Binding Sites. *Magnetochemistry* **2018**, *4*, 55.
(64) Bjørklund, G.; Dadar, M.; Pivina, L.; Doşa, M. D.; Semenova, Y.; Aaseth, J. The Role of Zinc and Copper in Insulin Resistance and Diabetes Mellitus. *Curr. Med. Chem.* **2020**, *27*, 6643−6657.
(65) Lowe, J.; Taveira-da-Silva, R.; Hilário-Souza, E. Dissecting Copper Homeostasis in Diabetes Mellitus. *IUBMB Life* **2017**, *69*, 255−262.
(66) Tanaka, A.; Kaneto, H.; Miyatsuka, T.; Yamamoto, K.; Yoshiuchi, K.; Yamasaki, Y.; Shimomura, I.; Matsuoka, T. A.; Matsuhisa, M. Role of Copper Ion in the Pathogenesis of Type 2 Diabetes. *Endocr. J.* **2009**, *56*, 699−706.
(67) Kim, S.; Kang, S. Serum Albumin Levels: A Simple Answer to a Complex Problem? Are We on the Right Track of Assessing Metabolic Syndrome? *Endocrinol. Metab.* **2013**, *28*, 17.
(68) Jun, J. E.; Lee, S. E.; Lee, Y. B.; Jee, J. H.; Bae, J. C.; Jin, S. M.; Hur, K. Y.; Lee, M. K.; Kim, J. H. Increase in Serum Albumin Concentration Is Associated with Prediabetes Development and Progression to Overt Diabetes Independently of Metabolic Syndrome. *PLoS One* **2017**, *12*, No. e0176209.
(69) Gu, S.; Wang, A.; Ning, G.; Zhang, L.; Mu, Y. Insulin Resistance Is Associated with Urinary Albumin-Creatinine Ratio in Normal Weight Individuals with Hypertension and Diabetes: The REACTION Study. *J. Diabetes* **2020**, *12*, 406−416.

https://doi.org/10.1021/jacs.3c04599
J. Am. Chem. Soc. 2023, 145, 16726−16738